Progress In Electromagnetics Research M, Vol. 79, 41–49, 2019

Polarization-Insensitive Frequency-Selective Rasorber Based on Square-Loop Element

Qiang Chen, Min Guo, Di Sang, and Yunqi Fu*

Abstract—This paper presents a polarization-insensitive frequency selective rasorber which has high in-band transmission at high frequency and wideband absorption at low frequency based on square-loop and parallel LC resonance. The rasorber consists of a bandpass FSS and a resistive sheet plus a slot-type metallic four-legged loaded element as the bandpass FSS element. The resistive element is realized by inserting several strip-type parallel LC structures into a resistor-loaded square-loop element, which allows the surface current to be controlled as necessary and the wave at the resonance frequency to be passed with minimum insertion loss. Wideband absorption is realized at low frequency, where the bandpass FSS is nearly totally reflected, and the FSR performs as an absorber. Simulation results show the transmission band at 9.9 GHz with transmissivity higher than 96% and the absorption band with absorptivity higher than 85% from 2.83 GHz to 8.6 GHz for TE-polarized 30° incidence and from 3.22 GHz to 8.48 GHz for TM-polarized 30° incidence. The absorptive/transmissive performance of the FSR structure is also verified by experimental measurements.

1. INTRODUCTION

Low-observable radome with absorption properties is a useful component in antenna systems, as they reduce out-of-band scattering when being exposed to detecting waves [1, 2]. The incident power from any enemy's radar system is absorbed by the lossy materials in the radome rather than reradiated or scattered. A radome structure can be realized by a frequency selective rasorber (FSR) [3] composed of a frequency selective surface (FSS) and resistive sheet. The FSS should be transmissive at the operating frequency of the hosted antenna. The resistive sheet, together with the bandpass FSS, absorbs the out-of-band incident wave over the FSS rejection band in a manner similar to a circuit analog absorber (CAA) [4].

The CAA is a periodical structure formed by placing resistive FSSs in front of a ground plane to absorb incident waves. Generally, the CAA only requires that the resistive sheet is matched with the impedance of free space. The resistive square loop (SL) is one of the most often-used elements in CAA design. It is polarization-insensitive and can realize wideband absorption through lossy film [5, 6] or loading lumped resistors [7–10]. A well-designed FSR must possess a low insertion loss at the transmission band apart from the wideband absorptive properties, however, which means that the resistive sheet must be nearly transparent at the operating frequency with minimum insertion loss. In other words, conventional resistive SL elements are not appropriate for FSR resistive sheets due to their high insertion loss. Many previous researchers have attempted to design FSR structures with absorptive/transmissive properties [2, 3, 11–18]. Some FSR structures have transmission bands below their absorption bands [2, 11–14], the resistive sheets of which are realized via resistive loop elements [2], lumped-resistor-loaded elements [11, 14], magnetic lossy materials [12], or even 3D lossy structures [13].

Received 6 November 2018, Accepted 16 January 2019, Scheduled 13 February 2019
* Corresponding author: Yunqi Fu (yunqifu@nudt.edu.cn).
The authors are with the College of Electronic Science, National University of Defense Technology, Changsha 410073, China.

An FSR with transmission band above the absorption band is actually preferable in terms of protecting the airborne antenna from detection by ground radar systems.

Several such FSR designs have been proposed [15–17]. A transmission band at 21 GHz and an absorption band over 5–13 GHz can be realized by a metamaterial structure, but the insertion loss is higher than 1.2 dB, and the absorption is low [15]. Several FSR designs can also realize a transmission band at high frequencies based on modified dipole elements, which are initially polarization-sensitive [16, 17]. A novel approach to producing a transmission band within a wide absorption band on the basis of elaborate design of equivalent circuit has also been proposed [3].

In this paper, we present a new FSR design characterized by a transmission band above a wideband absorption band based on an approach that we described in a previously published paper [18]. It also consists of a resistive sheet and a bandpass FSS. The element in the resistive sheet is realized by modifying a conventional lumped-resistor-loaded SL element. By inserting a strip-type parallel LC (PLC) structure into each side of the resistive SL element, it is made nearly transparent at the parallel resonance frequency with minimum insertion loss regardless of the ohmic loss by the lumped resistors. Below the parallel resonance frequency, the entire resistive SL element receives and dissipates the incident wave together with the bandpass FSS as a ground plane. A high in-band transmission at 9.9 GHz and a wideband absorption at low frequency can be successfully obtained through this design, as discussed in detail below.

2. DESIGN OF RESISTIVE SQUARE-LOOP ELEMENT

The resistive SL element, either by lossy film [5, 6] or by loading lumped resistors in metallic SL [7–10], has been extensively researched in regards to wideband absorption and low CAA profile. In previous studies, only the reflection and absorption performances of the resistive SL element are investigated; no researcher to date has analyzed the corresponding transmission performance. To design an FSR with low insertion loss at the transmission band, the insertion loss of the resistive sheet must be effectively optimized.

We first investigated the frequency response of two conventional resistive SL elements by loading lumped resistors or lossy film. The two resistive SL elements, along with their equivalent circuit, are depicted in Fig. 1. They have the same dimensions, $D = 11.4$ mm and $w = 1$ mm, and periodicity, 13.5 mm. Their transmission coefficients over the band 0.5–12 GHz with different resistance values are shown in Fig. 2. As the surface resistance and resistor varies, the transmission coefficient of the two SL elements exceeds -1 dB only at frequencies below 1 GHz and cannot exceed -4 dB from 6 GHz to 12 GHz. In short, the two conventional resistive SL elements can only be used to achieve a high in-band transmission below the absorption band [2, 11] and cannot realize a transmission band above the absorption band due to the high insertion loss at high frequency.

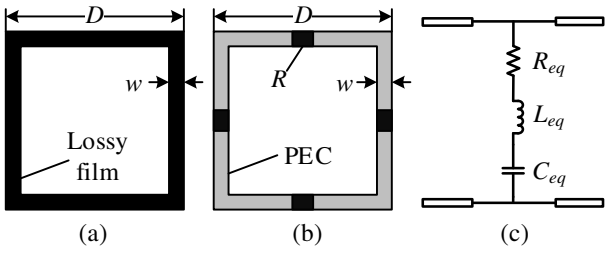

Figure 1. Unit cells of resistive SL element by (a) lossy film (b) loading lumped resistors and (c) their equivalent circuit.

In order to obtain a high in-band transmission at high frequency and ensure wideband absorptive performance at low frequency, we modified a conventional resistive SL element by introducing several PLC structures into a lumped-resistor-loaded metallic SL element. This formed a parallel LC that is cascaded with the series RLC in its equivalent circuit model. The capacitor was realized by a parallel-strip and the inductor by a meander strip. The modified resistive SL element and its equivalent circuit model are shown in Fig. 3. There is one strip-type PLC structure inserted in each side and a lumped

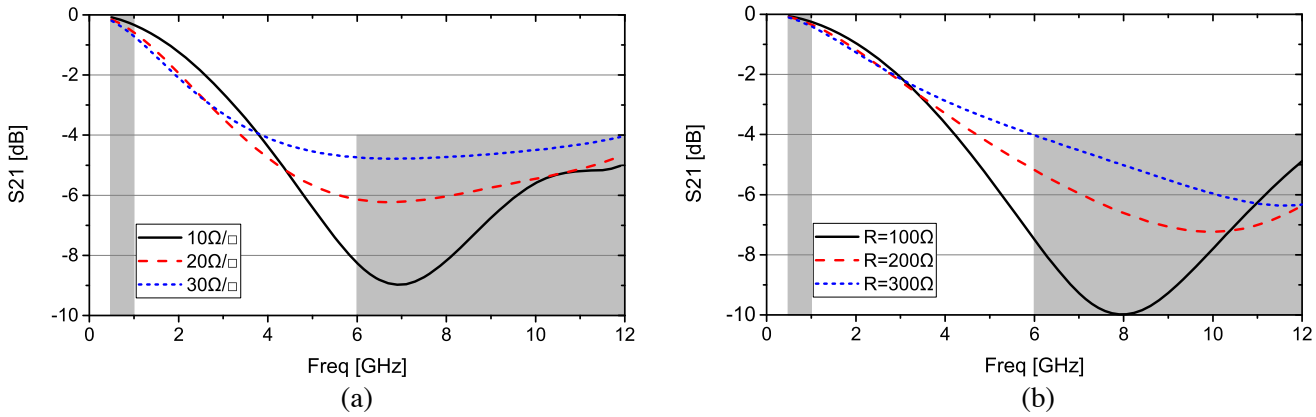

Figure 2. Transmission coefficients of the resistive SL FSS (a) lossy film and (b) loading lumped resistors with different resistance values.

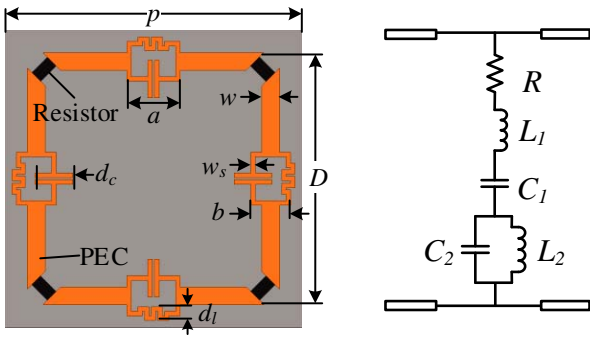

Figure 3. Resistive SL element inserted with strip-type PLC structures and lumped resistors.

resistor in each corner of the metallic SL. It can be modeled by a series RL_1C_1 cascaded with a parallel L_2C_2.

The equivalent impedance of the resistive SL element can be represented by:

$$Z_{SL} = R - j\frac{1-\omega^2 L_1 C_1}{\omega C_1} + j\frac{\omega L_2}{1-\omega^2 L_2 C_2} \tag{1}$$

The resonance frequency of the parallel L_2C_2 is:

$$f_h = \frac{1}{2\pi\sqrt{L_2 C_2}} \tag{2}$$

At f_h, the imaginary part of Z_{SL} resonates to infinity so that the resistive sheet is open-circuited, and the incident wave can be passed. The transmission frequency is only determined by the PLC structure. Below f_h, the parallel L_2C_2 is finitely inductive. The impedance Z_{SL} is in series resonance at a certain low frequency f_l, where the imaginary part becomes zero. The incident wave can be absorbed by the resistors.

To obtain a transmission band at 10 GHz and a wide absorption at low frequency, the dimensions of the resistive element were optimized as follows: $p = 13.5$ mm, $D = 11.4$ mm, $w = 1$ mm, $w_s = 0.1$ mm, $a = 2.4$ mm, $b = 1.8$ mm, $d_c = 1.7$ mm, $d_l = 0.6$ mm. The dielectric substrate supporting the resistive sheet is F4BM with thickness of 0.25 mm and $\varepsilon_r = 2.65$, $\tan\delta = 0.001$.

The transmission coefficients of the resistive sheet for different resistance values are simulated by HFSS and shown in Fig. 4(a). The distance of the resistive sheet to the PEC ground plane is 12 mm. It can be seen that a transmission band with minimum insertion loss is produced at 10 GHz for different resistance values. The stability of the transmission band as the function of resistance value is excellent.

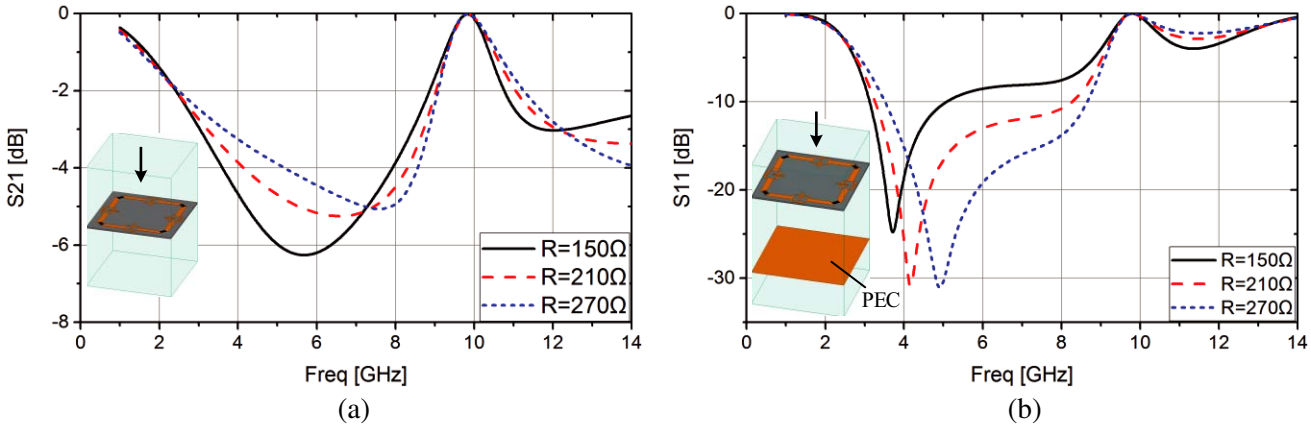

Figure 4. (a) Transmission coefficient of the resistive sheet; (b) reflection coefficient of the PEC-grounded resistive sheet.

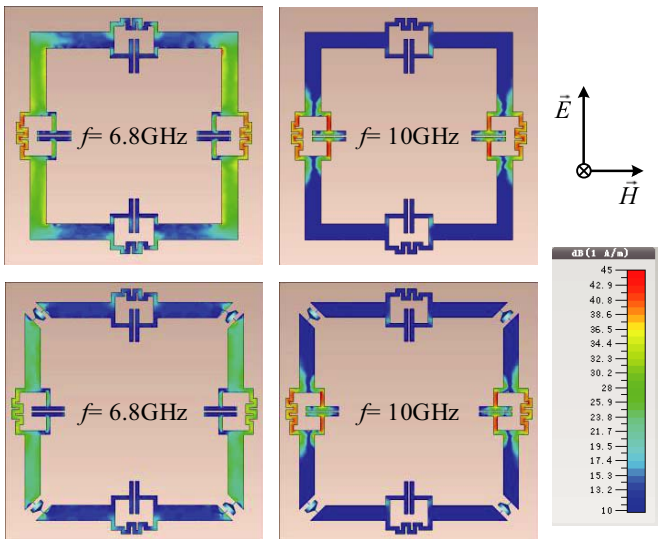

Figure 5. Surface current distribution of the PLC-loaded SL element without/with lumped resistors at 6.8 GHz and 10 GHz.

The PEC ground plane can be transformed into an absorber by placing it under the resistive sheet in such a way that incident waves can only be absorbed and reflected. The reflection coefficients of the absorber for different lumped resistor resistance values are shown in Fig. 4(b). As the resistance increased from 150 Ω to 270 Ω, the absorption peak shifted to a higher frequency, and the absorption grew stronger while the absorption bandwidth decreased. The reflection coefficient at 10 GHz remained stable because the resistive sheet was nearly transparent at this frequency, and no incident power was absorbed. In a word, the resistance value in the proposed design does not affect the transmission performance, only the absorptive performance. We set the resistance to 210 Ω in all the subsequent experiments described below.

To better understand the operating principle of the PLC structure, the surface current distribution in decibel scale of the PLC-loaded SL element without/with lumped resistors under a vertical-polarized incident wave at two frequencies (6.8 GHz, 10 GHz) as shown in Fig. 5. Only two PLC structures in the sides of the SL element parallel with the E-field of the incident wave perform parallel resonance. For the lossless element without lumped resistors, a surface current was intensively induced at two PLC structures at 10 GHz to form a loop current but was relatively weak in the other part of the SL element. The whole SL element was blocked into several short sections in the view of the surface current. At

6.8 GHz, the impedance of the PLC structure is finitely inductive and performs as an an inductor. Surface current can be strongly induced in the whole element.

After loading lumped resistors in the corners, the loop current at 10 GHz remained with little consumption, while the surface current at 6.8 GHz was strongly dissipated due to ohm loss in the resistors. The effective absorption of incident waves at the low band can be achieved together with a ground plane. The performance of the resistive PLC-loaded SL element also appeared polarization-insensitive due to the symmetrical structure.

3. PERFORMANCE OF THE FSR

We used a slot-type four-legged loaded element [4] as the bandpass FSS of the FSR structure, as it has polarization-insensitive bandpass performance at the transmission band and a wide total-reflected band making it an effective ground plane for absorption. Fig. 6 shows its reflection/transmission coefficients under TE- and TM-polarized oblique incidence with different angles. Its periodicity is 9 mm. We designed its passband at 10 GHz with favorable stability under different incident angles. It also has a total-reflected band from 1 GHz to 8 GHz, where it can act as the ground plane for the resistive sheet to absorb incident waves. As the incident angle increases, the total-reflected bandwidth decreases under TE polarization but increases for TM polarization.

A unit cell of the FSR consisting of 2×2 of resistive SL elements and 3×3 metallic bandpass elements is depicted in Fig. 7. Its dimensions are as follows: $p_1 = 13.5$ mm, $p_2 = 9$ mm, $t = 12$ mm, $w_1 = 0.2$ mm, $w_2 = 0.7$ mm, $l = 7.2$ mm. The lumped resistors are with the resistance of 210 Ω.

Both the resistive sheet and bandpass FSS are nearly transparent at the transmission band, thus an incident wave can pass through both layers with low insertion loss. At the rejection band of the bandpass

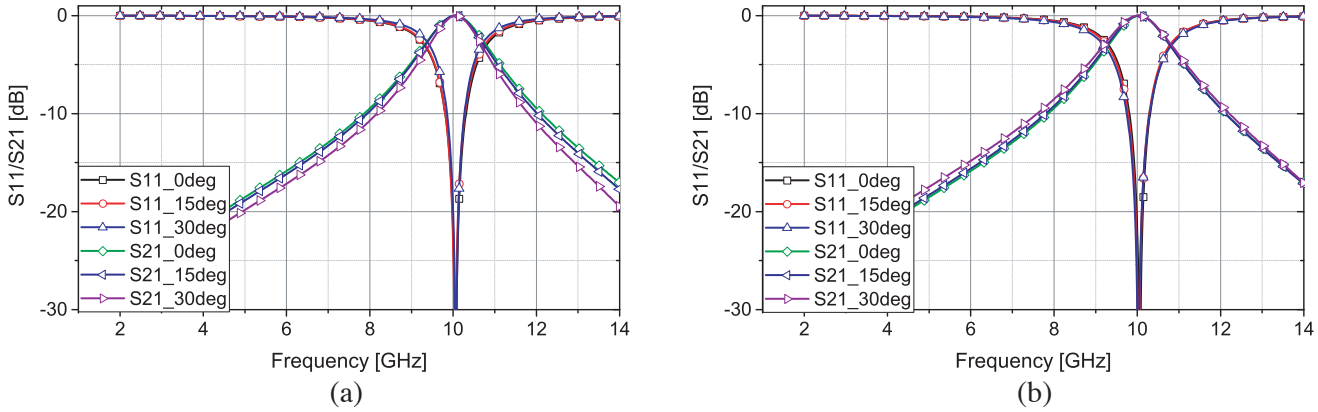

Figure 6. Reflection/transmission coefficients of slot-type four-legged element under (a) TE- and (b) TM- polarized oblique incidence.

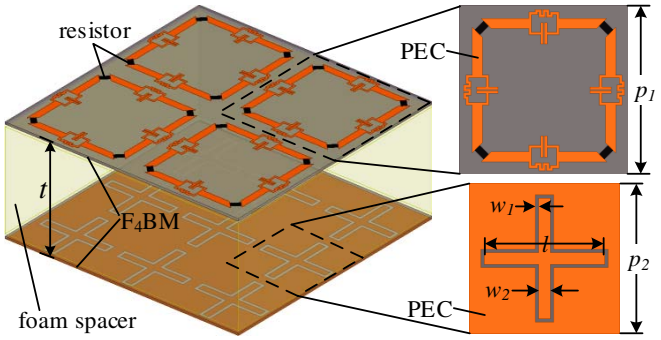

Figure 7. FSR unit cell consisting resistive SL elements and bandpass FSS.

FSS below 8 GHz, it is almost total-reflected and serves as a ground plane for the resistive sheet to absorb the incident wave. The absorptive performance is determined by the lumped resistor and the thickness between the resistive sheet and bandpass FSS. To assess the absorptive/transmissive performance of the FSR, we define absorptivity (A), reflectivity (R), and transmissivity (T) as the absorption rate and the transmission rate of the incident power, which can be expressed by the S-parameter results:

$$\begin{aligned} R &= |S_{11}|^2, T = |S_{21}|^2 \\ A &= 1 - R - T = 1 - |S_{11}|^2 - |S_{21}|^2 \end{aligned} \tag{3}$$

The absorptivity and transmissivity of the FSR structure under TE-and TM-polarized incident waves with different incident angles, together with the absorptivity of the PEC-grounded absorber shown in Fig. 4(b) with resistance of 210 Ω, were analyzed by HFSS as shown in Fig. 8. A plane wave was illuminated on the resistive side of the FSR with a transmission band located at 10 GHz, which is almost independent of the incident polarizations and angles. The stability of the transmission band as a function of incident polarizations and angles is excellent because the transmission performance of the resistive sheet is mainly determined by the strip-type PLC structure, which approximates lumped elements owing to the PLC dimensions of 2.4 mm, i.e., less than 0.1λ at 10 GHz. The bandpass FSS also has a stable transmission band. The transmissivity peaks in all cases were greater than 96%.

The absorption bandwidth under normal incidence with absorptivity greater than 85% covers the band 2.83–8.67 GHz, and the transmission band is at 10 GHz with insertion loss of 0.12 dB. Under oblique incidence up to 30°, the absorption band is 2.83–8.6 GHz for TE polarization and 3.22–8.48 GHz for TM polarization. The absorption band of the PEC-grounded absorber under normal incidence extended from 3.27 GHz to 8.27 GHz. The absorption bandwidth of the FSR under most of the simulated cases was as wide as the absorber structure, indicating that the bandpass FSS performs well as the ground plane at low frequency, and the FSR has absorption performance as good as the absorber structure. The absorption performance at low frequency and the transmission performance at high frequency of the FSR were nearly independent of each other in our simulation. Table 1 shows the performance comparison of this work and other FSR designs in the literature. Compared to other FSR designs, this work features wider absorption band and polarization-insensitive absorption/transmission performance.

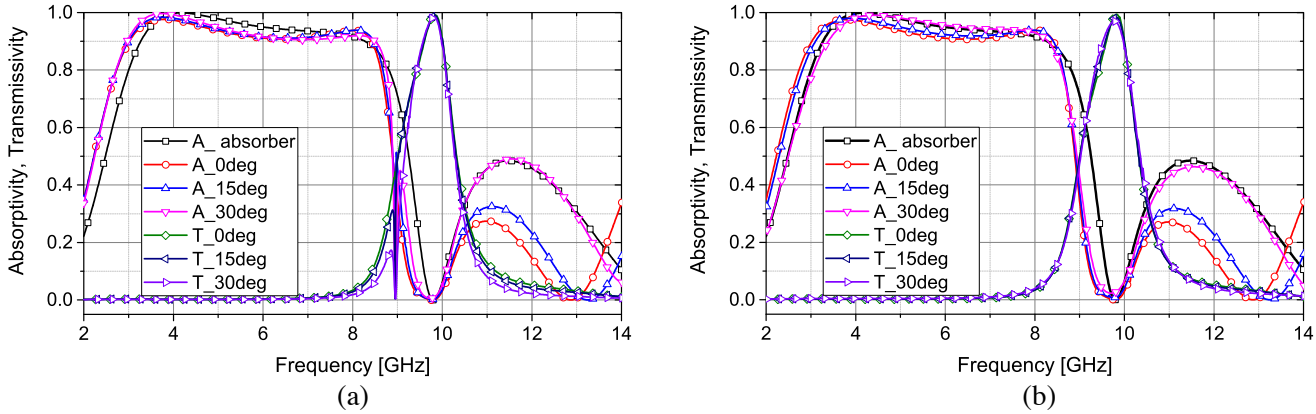

Figure 8. Simulated absorptivity and transmissivity of FSR structure under (a) TE-and (b) TM-polarized incident wave with different incident angles. PEC-grounded absorber (Fig. 4(b)) absorptivity with resistance of 210 Ω under normal incidence also provided in each figure as "A_absorber" for comparison.

4. EXPERIMENT AND DISCUSSION

We built a prototype of the FSR 300 mm × 300 mm in size to verify the absorptive/transmissive performance of the polarization-insensitive FSR by experimentation. The prototype contains 22×22 resistive SL elements and 33×33 bandpass FSS elements. Both the resistive sheet and bandpass FSS

Table 1. Performance comparison of FSR designs.

Ref.	Polarization	Absorption band	Transmission band
[2]	Dual	10–18 GHz (57%)	4.6 GHz/0.3 dB
[11]	Dual	3–9 GHz (100%)	1 GHz/1 dB
[13]	Single	4.8–9.3 GHz (63.8%)	4.15 GHz/2.4 dB
[14]	Dual	3–9 GHz (100%)	1 GHz/0.3 dB
[15]	Dual	5.5–13 GHz (81%)	21 GHz/1.2 dB
[16]	Single	2.8–8.3 GHz (99.1%)	9.7 GHz/0.5 dB
[17]	Single	2.7–8.3 GHz (101.8%)	9.45 GHz/1.5 dB
[18]	Dual	3–9 GHz (100%)	10 GHz/0.2 dB
This work	Dual	2.83–8.67 GHz (101.6%)	10 GHz/0.12 dB

were printed on a thin F4BM dielectric substrate with $\varepsilon_r = 2.25$ and thickness of 0.25 mm via print circuit board technology. Four lumped resistors (210 Ω) with 0603 package are soldered on the corners of each resistive SL element. The resistive sheet and bandpass FSS were fixed on different sides of a polymethacrylimide (PMI) foam spacer with 11.5 mm thickness by nylon screws. The total thickness of the FSR prototype is 12 mm. The prototypes of the resistive sheet and the bandpass FSS are shown in Fig. 9.

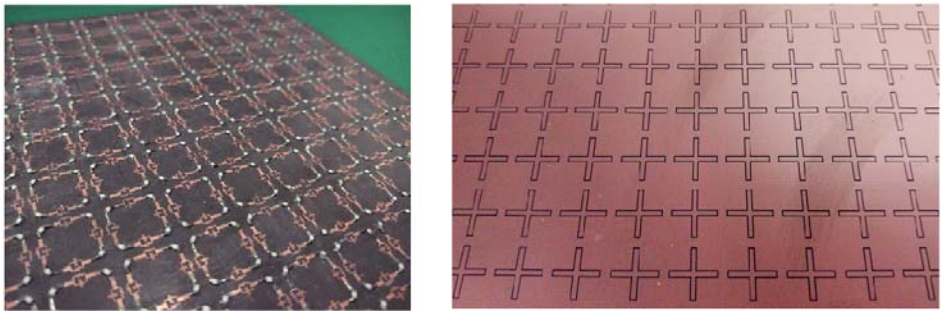

(a) (b)

Figure 9. FSR prototype (a) resistive SL sheet (b) bandpass FSS.

The absorptive/transmissive performance of the FSR prototype was measured in an anechoic chamber using a free-space measurement setup. The measurement setup is similar to that presented in [14].

The measured and simulated reflection/transmission coefficients under TE- and TM-polarized oblique incidences up to 30° are shown in Fig. 10. The simulated transmission band is at 9.9 GHz showing insertion loss less than 0.2 dB for all the simulated cases. In the measured results, the transmission band shifted to 10.3 GHz with insertion loss less than 0.5 dB and remained stable under different polarizations and incident angles. This frequency shift was caused by fabrication error in the prototype. As the frequency decreased, the transmission coefficients increased at frequencies below 6 GHz because the electrical size of the prototype was smaller at lower frequency so that more incident power from the transmitting antenna was diffracted to the receiving antenna.

Wideband absorption for both TE and TM polarizations was observed from both the simulated and measured results. The simulated absorption band with reflection coefficients lower than −9 dB extended from 3.3 GHz to 8.3 GHz in all the cases. The measurements are roughly consistent with the simulated results despite some slight disagreement which, again, we attribute to fabrication error and experimental conditions.

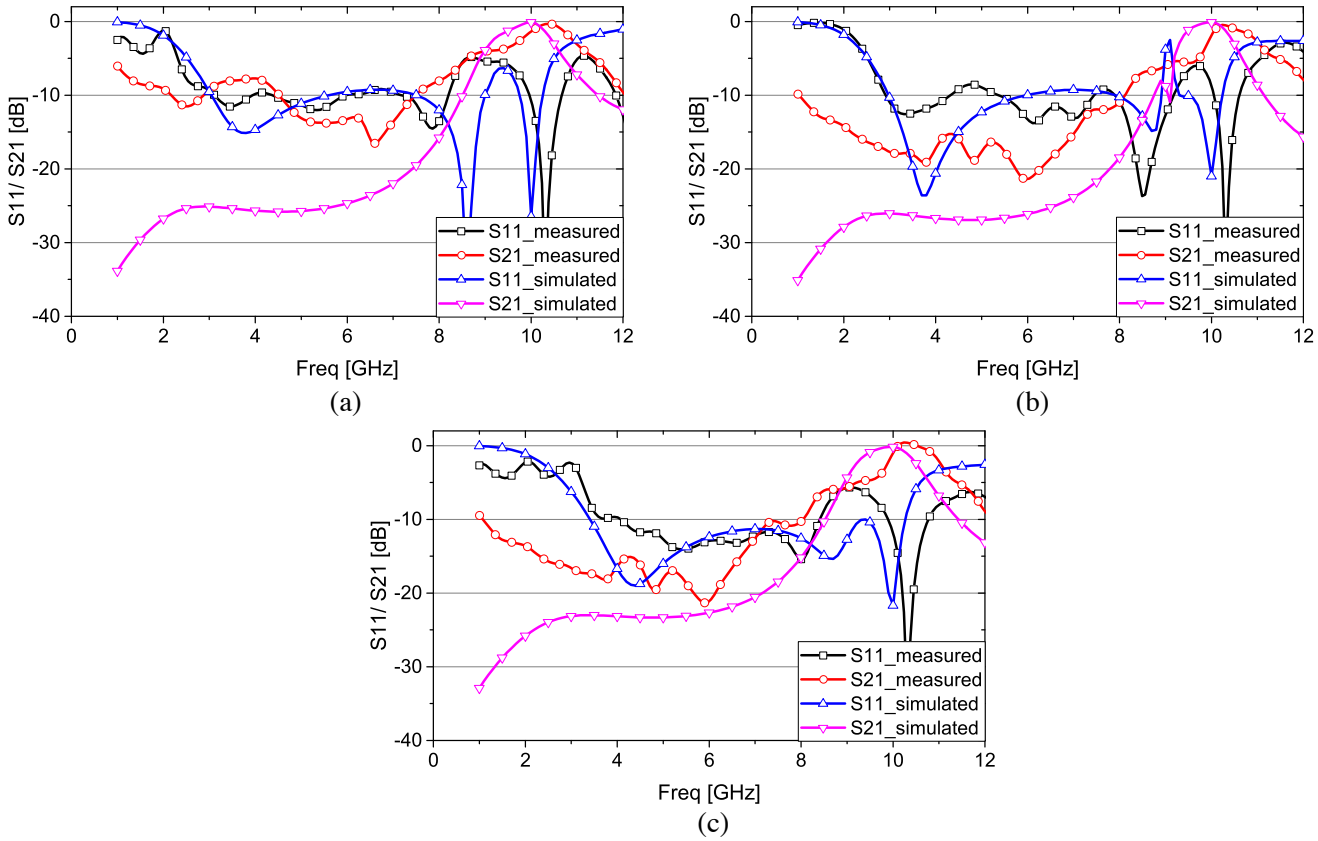

Figure 10. Measured reflection/ transmission coefficients of the FSR prototype and the simulated results (a) normal incidence, (b) TE-polarized 30° incidence, (c) TM-polarized 30° incidence.

5. CONCLUSION

A polarization-insensitive FSR structure composed of a PLC-based resistive sheet and a bandpass FSS was designed and assessed in this study. The proposed structure has a high in-band transmission at high frequencies and a wideband absorption at low frequencies. The PLC-based resistive sheet, unlike conventional resistive sheets which only have absorptive performance at the absorption band, has minimum insertion loss at the transmission band. The bandpass FSS, an array of slot-type four-legged loaded elements, also showed stable bandpass performance. The FSR structure has a transmission band at 9.9 GHz with transmissivity greater than 96%, which is almost independent of the polarizations and angles of the incident wave. The absorption band has absorptivity higher than 85% from 2.83 GHz to 8.6 GHz under TE-polarized 30° incidence and from 3.22 GHz to 8.48 GHz under TM-polarized 30° incidence. We also fabricated a prototype of the proposed design and verified its absorptive/transmissive performance experimentally.

REFERENCES

1. Munk, B. A., *Metamaterials: Critique and Alternatives* , Wiley, New Jersey, 2009.
2. Costa, F. and A. Monorchio, "A frequency selective radome with wideband absorbing properties," *IEEE Trans. Antennas Propag.*, Vol. 60, No. 6, 2740–2747, 2012.
3. Shang, Y. P., Z. X. Shen, and S. Q. Xiao, "Frequency-selective rasorber based on square-loop and cross-dipole arrays," *IEEE Trans. Antennas Propag.*, Vol. 62, No. 11, 5581–5589, 2014.
4. Munk, B. A., *Frequency Selective Surfaces: Theory and Design* , Wiley, New York, 2000.

5. Costa, F., A. Monorchio, and G. Manara, "Analysis and design of ultra-thin electro-magnetic absorbers comprising resistively loaded high impedance surfaces," *IEEE Trans. Antennas Propag.*, Vol. 58, No. 5, 1511–1558, 2010.
6. Li, M., S. Xiao, Y. Bai, and B. Wang, "An ultrathin and broadband radar absorber using resistive FSS," *IEEE Antennas Wireless Propag.*, Vol. 11, 748–751, 2012.
7. Han, Y., W. Che, C. Christopoulos, Y. Xiong, and Y. Chang, "A fast and efficient design method for circuit analog absorbers consisting of resistive square-loop arrays," *IEEE Trans. Electromagn. Compat.*, Vol. 58, No. 3, 747–757, 2016.
8. Shang, Y., Z. Shen, and S. Xiao, "On the design of single-layer circuit analog absorber using double-square-loop array," *IEEE Trans. Antennas Propag.*, Vol. 61,No. 12, 6022–6029, 2013.
9. Yang J. and Z. Shen, "A thin and broadband absorber using double-square loops," *IEEE Antennas Wireless Propag. Lett.*, Vol. 6, 388–391, 2007.
10. Ghosh, S., S. Bhattacharyya, and K. V. Srivastava, "Design, characterisation and fabrication of a broadband polarisation-insensitive multi-layer circuit analogue absorber," *IET Microw, Antennas Propag.*, Vol. 10, No. 10, 850–855, 2016.
11. Liu, L. G., P. F. Guo, J. J. Huang, W. W. Wu, J. J. Mo, Y. Q. Fu, and N. C. Yuan, "Design of an invisible radome by metamaterial absorbers loaded with lumped resistors," *Chin. Phys. Lett.*, Vol. 29, No. 1, 012101, 2012.
12. Zhou, H., L. Yang, S. Qu, K. Wang, J. Wang, H. Ma, and Z. Xu, "Experimental demonstration of an absorptive/ transmissive FSS with magnetic material," *IEEE Antennas Wireless Propag. Lett.*, Vol. 13, 114–117, 2014.
13. Li, B. and Z. X. Shen, "Wideband 3D frequency selective rasorber," *IEEE Trans. Antennas Propag.*, Vol. 62, No. 12, 6536–6541, 2014.
14. Chen, Q., J. J. Bai, L. Chen, and Y. Q. Fu, "A miniaturized absorptive frequency selective surface," *IEEE Antennas Wireless Propag. Lett.*, Vol. 14, 80–83, 2015.
15. Chen, X., Y. Q. Li, Y. Q. Fu, and N. C. Yuan, "Design and analysis of lumped resistor loaded metamaterial absorber with transmission band," *Opt. Express*, Vol. 20, No. 27, 28347–28352, 2012.
16. Chen, Q., L. Chen, J. J. Bai, and Y. Q. Fu, "Design of absorptive frequency selective surface with good transmission at high frequency," *Electron. Lett.*, Vol. 51, No. 12, 885–886, 2015.
17. Chen, Q., L. G. Liu, L. Chen, J. J. Bai, and Y. Q. Fu, "Absorptive frequency selective surface using parallel LC resonance," *Electron. Lett.*, Vol. 52, No. 6, 418–419, 2016.
18. Chen, Q., S. L. Yang, J. J. Bai, and Y. Q. Fu, "Design of absorptive/ transmissive frequency-selective surface based on parallel resonace," *IEEE Trans. Antennas Propag.*, Vol. 65, No. 9, 4897–4902, 2017.